Infrared Spectrum of the H_3N-HI Complex in Solid Ne, Ar, Ne/Ar, Kr, and N_2. Comparisons of Matrix Effects on Hydrogen-Bonded Complexes

Lester Andrews* and Xuefeng Wang

Department of Chemistry, University of Virginia, Charlottesville, Virginia 22904-4319

Received: March 29, 2001; In Final Form: May 22, 2001

Ammonia and hydrogen iodide vapors from the thermal decomposition of NH_4I were codeposited with excess neon at 5 K to form the H_3N-HI complex. New 630, 1192, and 3435 cm^{-1} infrared absorptions are assigned to the antisymmetric N−H−I stretching, symmetric NH_3 bending, and antisymmetric NH_3 stretching modes of the 1:1 complex. Vibrational assignments are supported by $^{15}NH_3$, ND_4I, and mixed H/D isotopic substitution. Complementary experiments were done with argon, neon/argon mixtures, krypton, and nitrogen to investigate the 1:1 complex in a range of matrix environments and to compare with previous work using the reagent gases. The above modes are shifted to 592, 1259, and 3400 cm^{-1} in solid argon owing to an increased interaction with the more polarizable argon matrix atoms. Neon and 2% argon mixtures gave intermediate absorptions, which evolved to the pure argon values on annealing to allow diffusion. The strong nitrogen matrix infrared absorption at 1955 cm^{-1} shifts approximately 4 cm^{-1} with ^{15}N-substitution, which suggests an N−H stretching mode and substantial proton transfer toward a more ionic complex in the nitrogen host. These and earlier matrix isolation experiments show that the matrix environment markedly affects the hydrogen bonding interaction and the degree of proton transfer in this polar H_3N-HI hydrogen-bonded complex.

Introduction

Ammonia complexes with HF, HCl, HBr, and HI are important models for the investigation of hydrogen bonding and host matrix effects because they exhibit simple diagnostic physical properties and decreasing HX ionic dissociation energies. These complexes have been examined by quantum chemical calculations,[1−4] by matrix infrared spectroscopy,[5−11] and by microwave spectroscopy in a supersonic jet.[12−15] Although each H_3N-HX complex is characterized as a simple molecular complex in the gas-phase ground vibrational state, there is evidence in the nitrogen nuclear quadrupole coupling constants for a very small amount of ionic character, which increases in the above series.[15,16] The infrared spectrum also examines the first excited vibrational state, which will be more anharmonic and more ionic and will interact more with a matrix host in the above order. Accordingly, matrix infrared spectra of H_3N-HF reveal a diagnostic H−F fundamental (3106 and 3041 cm^{-1} in neon and argon, respectively) which is slightly below the gas-phase value (3220 ± 10 cm^{-1}), but the H_3N-HCl complex exhibits widely differing H−Cl absorptions in solid neon (2084 cm^{-1}) and argon (1371 cm^{-1}), and the gas-phase infrared spectrum has not been recorded.[6,9,17−19] This trend is explained by the stronger interaction of the more polarizable argon matrix with the H_3N-HCl complex, which increases the degree of proton transfer. The three lighter H_3N-HX complexes have been examined by MP2 calculations, and increased anharmonicity in $v = 0$ and $v = 1$ levels and increased interaction with matrix hosts were noted for the above order.[20−22]

In view of the clear differences between argon and nitrogen matrix infrared spectra of H_3N-HI,[10,11] it is desirable to investigate this complex in the more inert neon matrix host. Furthermore, the value of ^{15}N substitution for characterizing the vibrational modes has been demonstrated for H_3N-HCl and H_3N-HBr.[19,23] We report here infrared spectra of the H_3N-HI complex in Ne, Ar, Kr, and N_2 matrices, a comparison of hydrogen bonding trends in the H_3N-HX model complex series, and evidence for more proton transfer in the more strongly interacting nitrogen matrix.

Experimental and Computational Section

Ammonia and hydrogen iodide vapors from thermal decomposition of solid NH_4I were codeposited with excess neon at 3 mmol/h onto a 5 K (Heliplex, APD Cryogenics) CsI window for two or three 30 min periods, and infrared spectra were recorded on a Nicolet 750 instrument at 0.5 cm^{-1} resolution. The solid NH_4I (Aldrich) was thoroughly degassed and heated externally to 110−140 °C in a Teflon bore right-angle valve (Ace Glass, 3 mm)-controlled sample tube with an 11 cm side arm through a vacuum fitting to a point 2 cm from the cold surface.[23,24] The internal side arm was heated to approximately 140 °C to prevent the condensation of solid NH_4I. The NH_3 concentration in the neon matrix is estimated to be about 0.2% from published spectra.[25] Ammonia and hydrogen iodide vapors were also codeposited with matrix gas samples containing approximately 0.2% $^{15}NH_3$ (99% ^{15}N, MSD Isotopes). A ND_4I sample was prepared by exchanging NH_4I with D_2O in the sample tube three times and evaporating residual D_2O at 40−50 °C, which serves to exchange deuterate the side arm and allow for the delivery of relatively pure DI and ND_3 into the matrix. A small mixed H/D sample was made from equal parts NH_4I and ND_4I in the sample tube.

Density functional theory (DFT) calculations[26] were used to predict frequencies for the H_3N-HCl and H_3N-HBr complexes.[19,23] The B3LYP and BPW91 functionals, 6-311++G-(d,p) basis sets, and LANL2DZ pseudopotential were employed.[27−30] All geometrical parameters were fully optimized, and harmonic vibrational frequencies were computed analytically at the optimized structures.

10.1021/jp011205c CCC: $20.00
Published on Web 07/20/2001

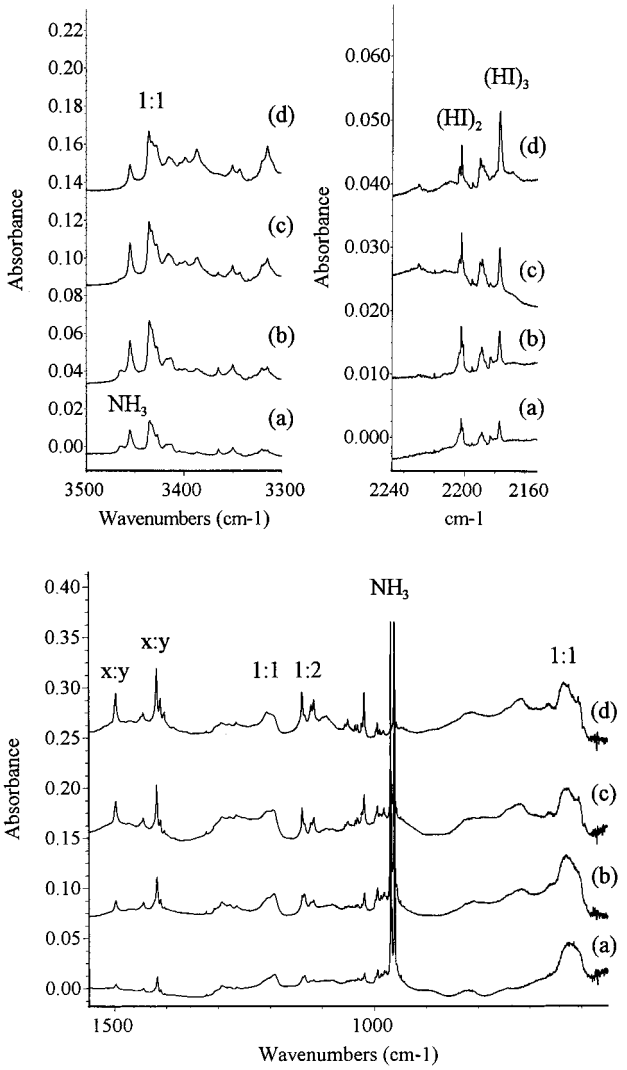

Figure 1. Infrared spectra in the 3500−3300, 2260−2140, and 1550−550 cm^{-1} regions for NH_4I vapors codeposited with neon at 5 K (a) after deposition for 60 min, (b) after deposition for 90 min, (c) after annealing at 10 K, and (d) after annealing at 12 K.

Results

Neon. Infrared spectra are shown in Figure 1 for 60 and 90 min NH_4I deposition periods and subsequent annealings to 10 and 12 K. The spectra of NH_3, $(NH_3)_2$, $(HI)_2$, and $(HI)_3$ are in agreement with previous reports based on reasonable argon−neon matrix shifts; note that HI is not detected owing to its very low infrared intensity.[25,31−34] The strongest new feature at 630 cm^{-1} is associated with new 1192.5 and 3435.3 cm^{-1} absorptions on deposition and annealing. Table 1 lists all of the observed bands. Annealing to 10 and 12 K had little effect on the 630, 1192.5, and 3435.3 cm^{-1} bands, but a sharp 1138.0 cm^{-1} band increased markedly, and 1418.2, 1444.6, and 1497.5 cm^{-1} bands increased. Diffusion on annealing cycles decreased the NH_3 monomer absorption and increased $(NH_3)_2$, $(HI)_2$, and $(HI)_3$ absorptions and also increased the broad 710 cm^{-1} band and other absorptions listed in Table 1. Experiments were done with different sample tube temperatures; increasing the sample temperature favored the bands that increased on annealing relative to the first product bands.

The above bands shifted in similar experiments using neon doped with $^{15}NH_3$ as shown in Figure 2 and listed in Table 1. With relatively pure isotopic ND_4I (note the weak, sharp NHD_2 band at 840.4 cm^{-1}), the primary bands were found at 473, 960.3, and 2558.3 cm^{-1} and the 876.5, 1079.1, and 1133.2 cm^{-1} bands increased on annealing as illustrated in Figure 3. One experiment with the mixed H/D sample gave 1192, 1130, and 1044 cm^{-1} bands in proportion to the ammonia precursors (the 960 cm^{-1} band was masked by NH_3), and a strong 630−600 cm^{-1} feature was observed.

TABLE 1: Infrared Absorptions (cm^{-1}) from Codeposition of Ammonia and Hydrogen Iodide Vapor from Ammonium Iodide with Excess Neon at 5 K

NH_4I	$^{15}NH_3$[a]	ND_4I	identification
3453.0	3444.6	2569.3	NH_3, ν_3
3435.3	3426.5	2558.3	H_3N-HI
3412.6	3404.4	2541.0	$(NH_3)_2$, "ν_3"
3364.3	3361.4	2420.7	NH_3, ν_1
3319.8	3314.9		$(NH_3)_2$, "ν_1"
2574.4		1964.3	$(NH_3)_x(HI)_y$
2558.1	2551.6	1934.2	$(NH_3)_x(HI)_y$
not obs	not obs	not obs	HI, R(0)
2203.0	2203.0	1578.4	$(HI)_2$
2171.3	2171.3	1552.0	$(HI)_3$
1988		1616	aggregate
1953		1604	aggregate
1644.8	1641.4	1199.9	NH_3, ν_4
1497.5	1492.2	1133.2	$(NH_3)_x(HI)_y$
1444.6	weak	1095.8	$(NH_3)_x(HI)_y$
1418.2	1412.3	1079.1	$(NH_3)_x(HI)_y$
1192.5	(1190)	960.3	H_3N-HI
1138.0	1132.8	876.5	$(H_3N)(HI)_2$
1115.5	1111.0	863.0	$(H_3N)(HI)_2$
1019.4	1014.7	793.1	$(NH_3)_3$
994.0	989.4	779.6	$(NH_3)_2$
968.2	964.1	767.4	NH_3, ν_2
960.7	956.6	757.0	NH_3, ν_2 site
810		610	$(NH_3)_x(HI)_y$
710		532	$(NH_3)_x(HI)_y$
630	626	473	H_3N-HI
607	601		H_3N-HI site

[a] NH_4I + Ne/$^{15}NH_3$ sample: resolved bands are given; unresolved bands are in parentheses.

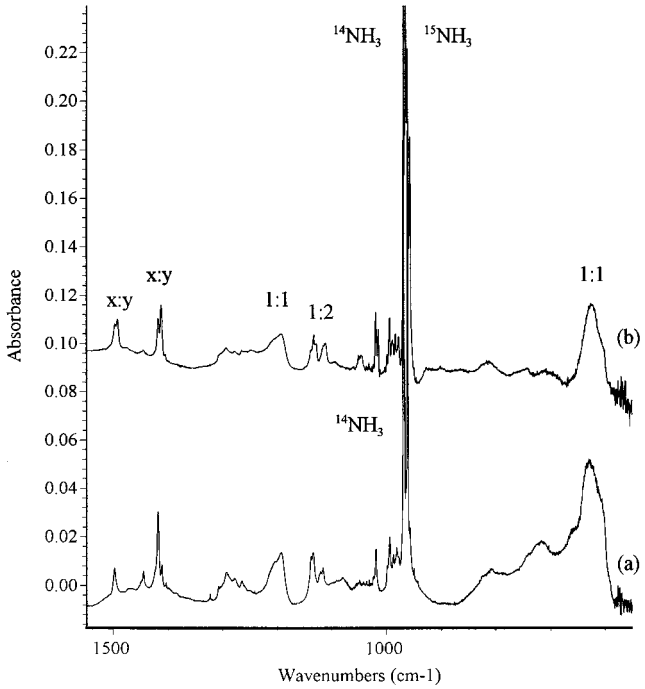

Figure 2. Infrared spectra in the 1550−550 cm^{-1} region for NH_4I vapors codeposited with neon at 5 K (a) after deposition for 90 min and (b) after codeposition of NH_4I vapors with neon containing 0.2% $^{15}NH_3$ for 60 min.

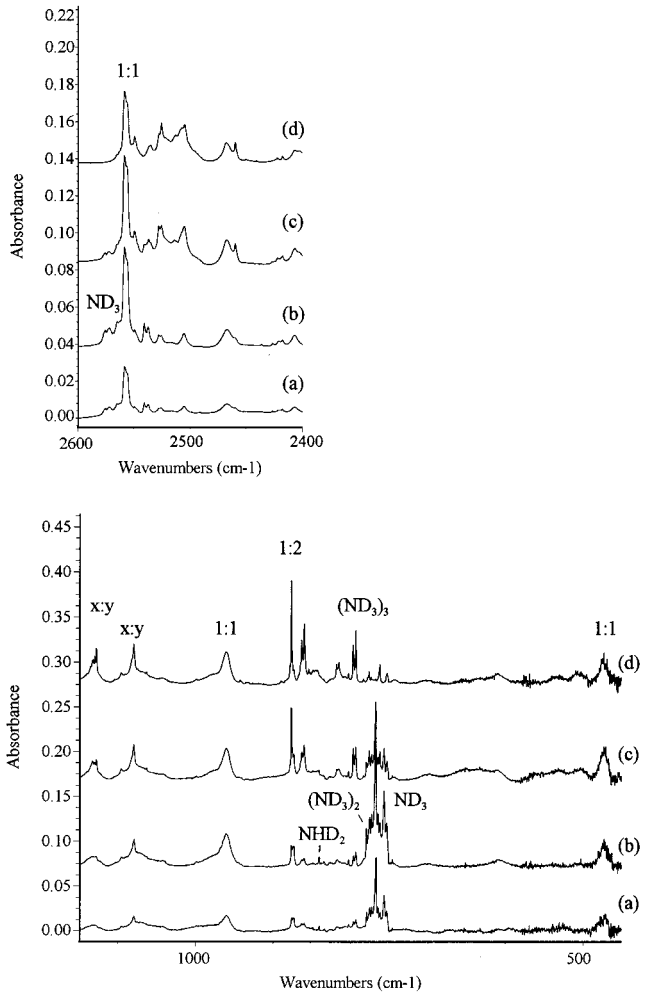

Figure 3. Infrared spectra in the 2600−2400 and 1150−450 cm^{-1} regions for ND_4I vapors codeposited with neon at 5 K (a) after deposition for 60 min, (b) after deposition for 90 min, (c) after annealing at 10 K, and (d) after annealing at 12 K.

Argon. Ammonium iodide experiments were done with argon condensed at 5 K. The HI monomer bands at 2253.8 and 2545.1 cm^{-1} and $(HI)_2$ at 2186.3 cm^{-1} were observed on deposition, and the $(HI)_3$ absorption appeared at 2153.8 cm^{-1} on annealing.[32−34] Figure 4 illustrates spectra for the natural isotopic sample in the 3500−2100 and 1700−500 cm^{-1} regions; note the sharp 999.9 cm^{-1} $(NH_3)_2$ band with 5% of the absorbance the NH_3 band at 974.6 cm^{-1}. The primary product absorptions at 3400.1, 1259, 875, and 592 cm^{-1} (labeled 1:1) are in excellent agreement with bands observed by Shriver et al.[10] and assigned to H_3N-HI. Annealing to 25 K has little effect on these absorptions, but weaker bands at 1497, 1442, 1417, 1401.8, 1126.9, and 680 cm^{-1} increase, and the latter bands increase further on 35 K annealing while the primary product bands decrease slightly. There is also small growth in $(HI)_2$ and $(NH_3)_2$ bands on annealing. A 40 K annealing decreases the primary bands more than the secondary set. The final annealing at 45 K (not shown) leaves little (about 5% of maximum intensity) of the above band and produces strong new ammonium iodide absorptions at 3123, 3023, 1685, and 1404 cm^{-1} in solid argon.[35,36] The above absorptions shifted with $^{15}NH_3$ added to the argon matrix gas as listed in Table 2.

Four experiments were performed with ND_4I substitution; the strongest product band is found at 1004 cm^{-1} in this work and at 1005 cm^{-1} in the work of Schriver.[11] We also observe new bands at 432 and 2534.2 cm^{-1} that track with the 1004 cm^{-1}

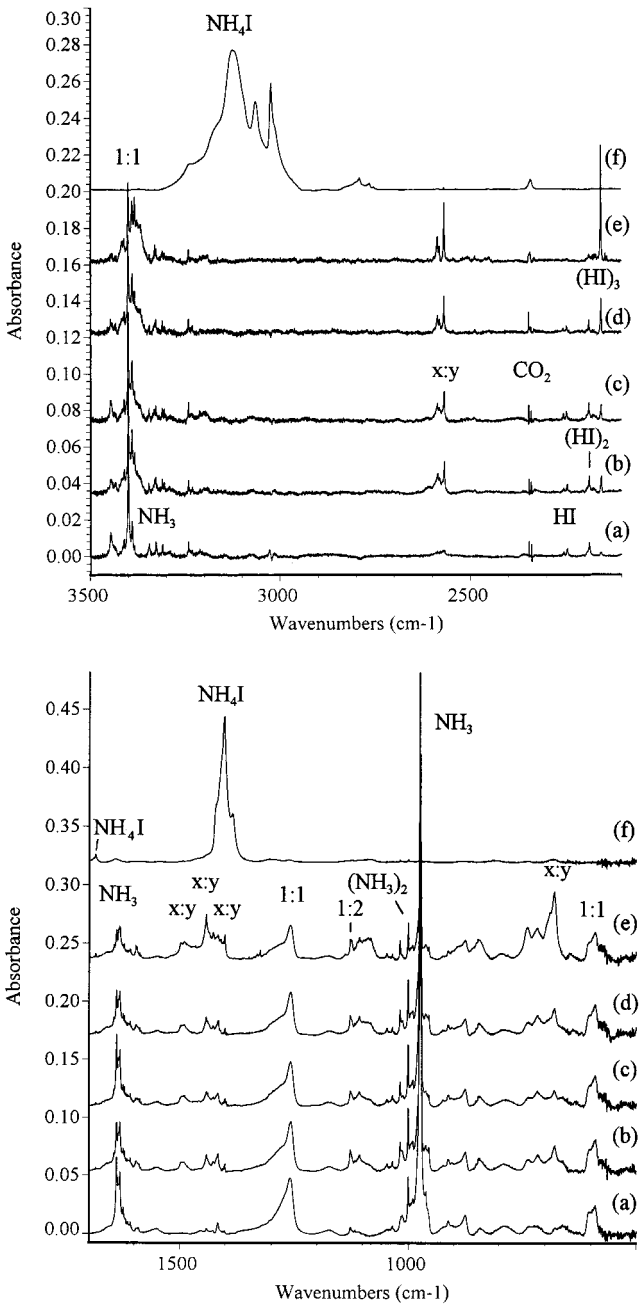

Figure 4. Infrared spectra in the 3500−2100 and 1700−500 cm^{-1} regions for NH_4I vapors codeposited with argon at 5 K (a) after deposition for 60 min, (b) after annealing at 30 K, (c) after irradiation at $\lambda > 240$ nm for 20 min, (d) after annealing at 35 K, (e) after annealing at 40 K, and (f) after annealing at 45 K.

absorptions; in more dilute samples, the 1312 cm^{-1} band increases on late annealing when the 1:1 complex absorptions decrease. Using 5 K deposition temperature, we observe sharp, weak 1614.4 and 1610.8 cm^{-1} bands that are probably due to DI in solid argon and a 1566.2 cm^{-1} $(DI)_2$ band; on annealing, the DI bands decrease, the $(DI)_2$ band increases, and a $(DI)_3$ band appears at 1544.5 cm^{-1}. To the best of our knowledge, DI monomer has not previously been detected in solid argon.[32−34] Sample codeposition at 6−8 K gave more precursor aggregation, poorer yield of 1:1 complex, and ND_4I absorptions. Finally, three experiments with mixed H/D samples gave four weak bands at 1255, 1138, 1081, and 1008 cm^{-1} that sharpened and then decreased like the 1:1 complex bands on annealing in the pure isotopic experiments.

TABLE 2: Infrared Absorptions (cm^{-1}) from Codeposition of Ammonia and Hydrogen Iodide Vapor from Ammonium Iodide with Excess Argon at 5 K

NH_4I	$^{15}NH_3$[a]	ND_4I	identification
3447.0	3439.0	2556	NH_3, ν_3
3400.1	3391.8	2534.2	H_3N-HI
3344.8	3342.0	2413	NH_3, ν_1
3310.3	3306.4		$(NH_3)_2$, "ν_1"
3123[b]		2340	NH_4I
3064[b]		2320	NH_4I
3023[b]		2233	NH_4I
2585.3	2580.0[c]	1971.2	$(NH_3)_x(HI)_y$
2567.9	2156.1[c]	1938.4	$(NH_3)_x(HI)_y$
2253.8	2253.8	1614.4	HI, R(0)
2245.1	2245.1	1610.8	HI site
2186.3	2186.3	1566.2	$(HI)_2$
2153.8	2153.8	1544.5	$(HI)_3$
1684.8		1299	NH_4I
1684.2	1678.0		$(NH_3)_x(HI)_y$
		1682	$(ND_3)_x(DI)_y$
1638.5	1635.3	1190.8	NH_3, ν_4
		1312	$(ND_3)_x(DI)_y$
1498.4	1492.4	1134.7	$(NH_3)_x(HI)_y$
1442.8	1437.0	1094.4	$(NH_3)_x(HI)_y$
1417.4	1411.8		$(NH_3)_x(HI)_y$
1404[b]		1064	NH_4I
1401.8	1395.6	1078.6	$(NH_3)_x(HI)_y$
1259	(1257)	1004	H_3N-HI
1127.1	1121.7	868.3	$(H_3N)(HI)_2$
1107.2	1102.7	852.9	$(H_3N)(HI)_2$
1018.0	1013.4	791.7	$(NH_3)_3$
999.9	995.3	780.4	$(NH_3)_2$
974.6	970.5	759.7	NH_3, ν_2
875	(874)		H_3N-HI
680	(679)	482	$(NH_3)_x(HI)_y$
606	603	442	H_3N-HI site
592	589	432	H_3N-HI site

[a] NH_4I + $Ar/^{15}NH_3$ sample: resolved bands are given; unresolved bands are in parentheses. [b] Features observed on final annealing; bands also observed at nearly the same wavenumber on window background with no matrix. [c] Broad triplet at 2583, 2582, 2580 cm^{-1} and sharp 1/2/1 triplet at 2567.9, 2564.8, 2561.5 cm^{-1}.

Neon/Argon Mixtures. Four experiments were performed with small amounts of argon added to neon to serve as a transition between the pure matrices. The first experiment with 5% Ar in Ne gave a slightly broadened version of the argon matrix spectrum with 1:1 complex bands at 3418, 1255, and 599 cm^{-1}; stepwise annealing shifted the upper band to 3406 and the 1255 cm^{-1} band to 1259 cm^{-1} with little effect on the lower band. Spectra from the 1% Ar in Ne investigation are compared with those of pure Ne and pure Ar matrices in Figure 5. The 1:1 complex absorptions are clearly broadened, and the upper two are shifted red to 3430 cm^{-1} and blue to 1207 cm^{-1} from neon values; stepwise annealing continues this trend shifting the bands to 3410, 1236, and 1256 cm^{-1} while the lower band forms peaks at 641 and 603 cm^{-1} (Figure 5b−e). A following experiment with 0.2% Ar in Ne gave new shoulders at 1210 and 601 cm^{-1} on the neon matrix bands (not shown). A study with 2% Ar in Ne gave new peaks at 3425, 1210, and 638 cm^{-1}, and annealing had essentially the same result (Figure 5f,g) as that seen with 1% Ar in Ne.

Krypton. Experiments were done with NH_4I and ND_4I in krypton containing 10% neon codeposited at 5 K followed by annealing at 20, 30, 40, and 50 K as described previously for NH_4Cl and NH_4Br.[19,23] New bands were observed at 3387, 1277, and 520 cm^{-1} after codeposition with NH_4I along with NH_3 bands and HI and $(HI)_2$ bands at 2232 and 2174 cm^{-1}. Annealing increased and then decreased the former bands, decreased HI and $(HI)_2$ bands, and produced a $(HI)_3$ band at 2149 and new higher cluster bands at 678, 1123.1, 1424.0, 1442.0, 1497.5, 2578.9, and 2592.7 cm^{-1}. New bands were observed at 2523 and 1038 cm^{-1} after codeposition with ND_4I along with ND_3 bands and DI and $(DI)_2$ bands at 1599.7 and 1557.8 cm^{-1}. Annealing decreased these bands and produced a $(DI)_3$ band at 1543.7 cm^{-1} and new higher cluster bands at 472, 866.0, 1078.5, 1093.3, 1133.0, 1945.4, and 1979.6 cm^{-1}.

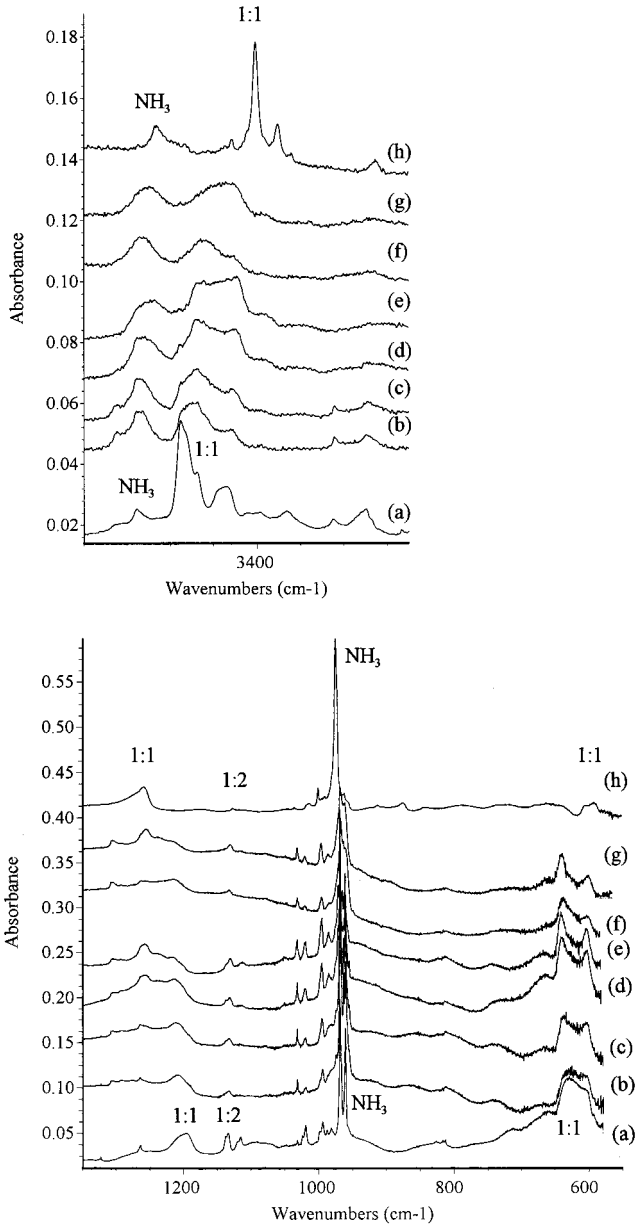

Figure 5. Infrared spectra in the 3480−3330 and 1350−550 cm^{-1} regions for NH_4I vapors codeposited with mixed neon/argon matrices at 5 K: (a) neon; (b) 1% argon in neon; (c) 1% argon in neon after annealing at 10 K; (d) 1% argon in neon after annealing at 12 K; (e) 1% argon in neon after annealing at 13 K; (f) 2% argon in neon; (g) 2% argon in neon after annealing at 10 K; (h) argon.

An experiment with NH_4I and pure Kr gave sharper bands and more light scattering than the above procedure, but essentially, the same frequencies were measured; HI gave two sites at 2240.0 and 2232.1 cm^{-1}, $(HI)_2$ absorbed at 2173.5 cm^{-1}, and $(HI)_3$ absorbed at 2148.8 cm^{-1}.

Nitrogen. Ammonium iodide vapors codeposited with excess N_2 at 5 K gave a spectrum containing ammonia and hydrogen iodide monomers and weak bands for the primary H_3N-HI complex (Figure 6) in essential agreement with that reported

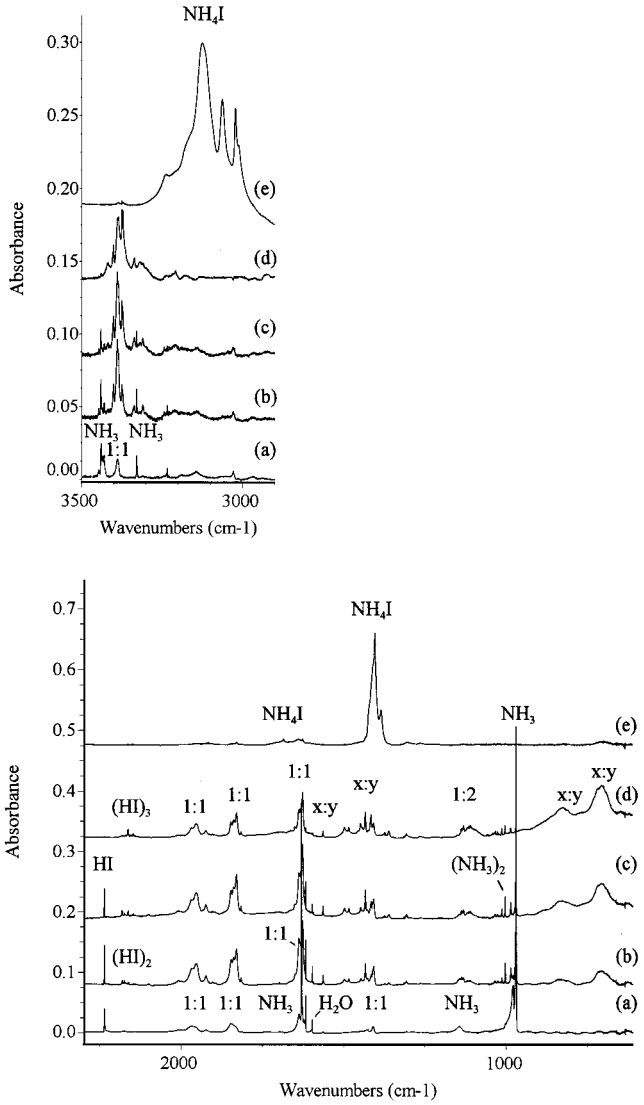

Figure 6. Infrared spectra in the 3500−2900 and 2300−600 cm^{-1} regions for NH_4I vapors codeposited with nitrogen at 5 K (a) after deposition for 60 min, (b) after annealing at 25 K, (c) after annealing at 32 K, (d) after annealing at 36 K, and (e) after annealing at 39 K.

by Schriver et al.[10] These bands increase on annealing, but bands for higher complexes increase more while the HI band decreases, the $(HI)_2$ band increases, and a $(HI)_3$ band appears.[37] The major 1:1 complex bands are 1967 and 1847 cm^{-1} on deposition, but annealing increases peaks at 1955 and 1831 cm^{-1} relatively more. Annealing at 36 K removes most of the ammonia and reduces the 1:1 complex absorptions, and a final annealing at 39 K converts most of the material back to NH_4I with absorptions listed in Table 2. In addition we obtained $^{15}NH_3$ counterparts for many absorptions as listed in Table 3.

Our ND_4I spectrum, Figure 7, is especially clean; after deposition, the 2237.0 cm^{-1} HI band is 0.0012 AU, the 1604.0 cm^{-1} DI band is 0.020 AU (considering oscillator strengths, our sample contains approximately 97% DI), and the 829.5 cm^{-1} NHD_2 band is 0.04 AU while the 759.0 cm^{-1} ND_3 band is 0.70 AU. Annealing at 25 K sharpened these bands to 2237.6 cm^{-1} (0.0033 AU) and 1604.4 cm^{-1} (0.061 AU) and produced the same 1:1 complex bands reported by Schriver, but our lower reagent concentrations allowed sharper absorptions to be measured and the strongest bands to be resolved at 1538.5 and 1527.6 cm^{-1} with a weaker hydrogen component at 1894.1 and 1886.0 cm^{-1}. Higher complex bands favored on annealing are

TABLE 3: Infrared Absorptions (cm^{-1}) from Codeposition of Ammonia and Hydrogen Iodide Vapor from Ammonium Iodide with Excess Nitrogen at 5 K

NH_4I	$^{15}NH_3$[a]	ND_4I	identification
3440.7	3432.5	2557.9	NH_3, ν_3
3402.3	3393.9	2530.8	$(NH_3)_2$, ν_3
3390.4	3382	2521.6	H_3N-HI
3330.4	3327.6	2415.5	NH_3, ν_1
3311.8	3307.7	2368.6	$(NH_3)_2$, "ν_1"
2729.7	weak	2064.1	$(NH_3)_x(HI)_y$
2712.8	weak	2030.7	$(NH_3)_x(HI)_y$
		1682	$(ND_3)_x(DI)_y$
2237.0	2237.0	1604.0	HI
2182.8	2182.8	1564.7	$(HI)_2$
2176.0	2176.0		$(HI)_2$
2165.5	2165.5	1553.2	$(HI)_3$
2163.3	2163.3	1551.9	$(HI)_3$
1967		1538.5	H_3N-HI site
1955	(1953)	1527.6	H_3N-HI
1925	1921		H_3N-HI site
1847			H_3N-HI site
1839			H_3N-HI site
1831	1831	1371.0	H_3N-HI
		1459.8	NHD_2
1637.9	1634.9		H_3N-HI site
1630.6	1627.5	1190.4	NH_3, ν_4
1626.7	1622.7	1254.3	H_3N-HI
1564.6	1553.8		$(NH_3)_x(HI)_y$
		1234.5	NHD_2
1498.3	1492.2	1133.3	$(NH_3)_x(HI)_y$
1484.2	1479.0	1117.9	$(NH_3)_x(HI)_y$
1434.0	1427.8	1088.8	$(NH_3)_x(HI)_y$
1408.6	1403.5	1068.0	H_3N-HI
		829.5	NHD_2
1137.4	1132.4	876.0	$(H_3N)(HI)_2$
1131.1	1126.0	870.9	$(H_3N)(HI)_2$
1003.4	998.9	781.8	$(NH_3)_2$
985.5	981.3	769.5	$(NH_3)_2$
969.6	965.2	759.0	NH_3, ν_2
829	(828)		$(NH_3)_x(HI)_y$
710	(709)	502	$(NH_3)_2(HI)$

[a] $NH_4I + N_2/^{15}NH_3$ sample: resolved bands are given; unresolved bands are in parentheses.

listed in Table 3. One mixed H/D experiment produced a 1/3/3/1 quartet of symmetric ammonia modes, a HI band at 2337.6 cm^{-1} (0.060 AU), a DI band at 604.4 cm^{-1} (0.15 AU), and a number of 1:1 complex bands that increased on annealing at 36 K and then gave way to ammonium iodide on annealing at 38 K (Figure 8). Our H/D spectra are a better resolved version of the bands of Schriver.[11] Annealing also produced broad 703 and 512 cm^{-1} bands.

Calculations. DFT calculations were done for the hydrogen-bonded H_3N-HI structure using the B3LYP and BPW91 functionals. The calculated N− I distances, 3.510 and 3.238 Å, respectively, are slightly shorter than the 3.584 Å microwave value.[14,15] Clearly, the BPW91 functional predicts a stronger hydrogen bonding interaction than the B3LYP functional, and both are considered as approximations for vibrational frequencies. Table 4 lists the results. The B3LYP functional also located an intermediate transition state and another minimum on the potential surface with a shorter (3.213 Å) N− I distance, larger dipole moment, and 0.63 kcal/mol higher energy. Computations for HI and NH_3 are given for comparison. In contrast, the reverse complex H_3N-IH (1.0141, 4.0981, 1.6073 Å bond lengths, no strong infrared bands, 2302 cm^{-1} (a_1, 11 km/mol)) is 5.8 kcal/mol higher in energy.

Calculations were done using the self-consistent isodensity polarized continuum model (SCIPCM)[38] for solvated molecules and the analytical option for frequency calculation in the

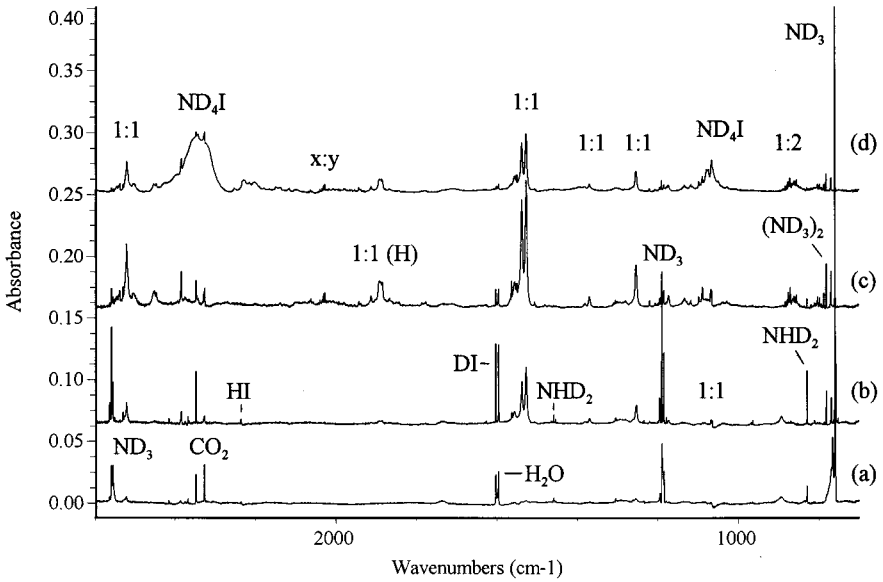

Figure 7. Infrared spectra in the 2600−700 cm^{-1} region for ND_4I vapors codeposited with nitrogen at 5 K (a) after deposition for 60 min, (b) after annealing at 25 K, (c) after annealing at 36 K, and (d) after annealing at 38 K.

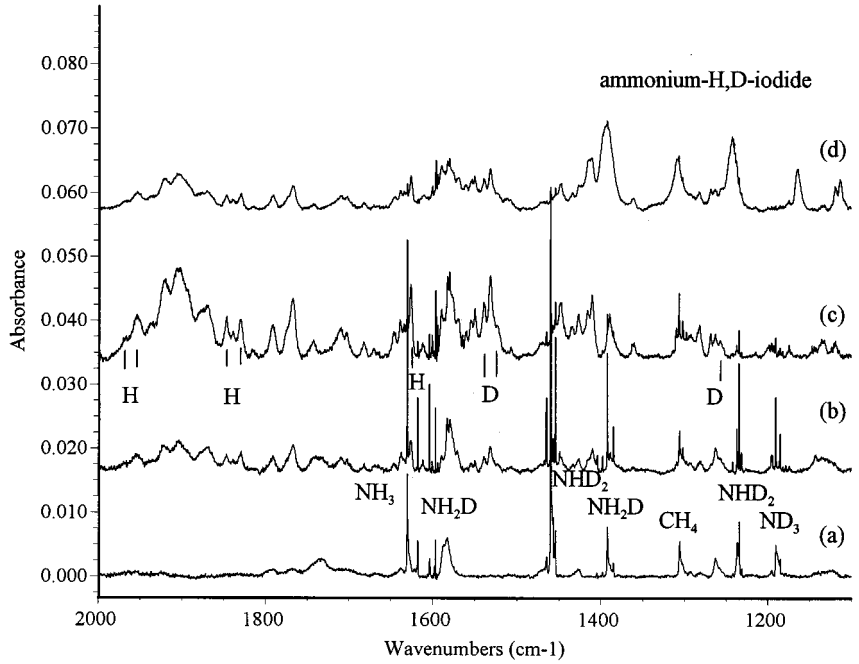

Figure 8. Infrared spectra in the 2000−1100 cm^{-1} region for mixed NH_4I/ND_4I vapors codeposited with nitrogen at 5 K (a) after deposition for 60 min, (b) after annealing at 25 K, (c) after annealing at 36 K, and (d) after annealing at 38 K. Pure H and D product absorptions are noted by short vertical lines.

Gaussian 98 program. This required a solvent, and heptane, which has the lowest dielectric constant (1.92) available, just larger than those of argon (1.63) and krypton (1.88), was employed. The solvent results for H_3N-HI are included in Table 4.

Discussion

The hydrogen-bonded complexes will be identified by annealing behavior and characterized by isotopic substitution in different matrix environments.

Argon. The H_3N-HI complex was first characterized by Schriver et al. in a seminal matrix isolation investigation of this difficult system.[10] Our experiments using NH_4I decomposition give lower reagent concentrations, and this, coupled with our lower 5 K deposition temperature, produces sharper product spectra favoring the 1:1 complex. We confirm assignment of the strongest bands for the 1:1 complex observed here at 3400, 1259, 875, and 592 cm^{-1} in solid argon. The sharp, weaker band observed here at 1401.8 cm^{-1} increases on annealing while the above 1:1 complex bands decrease, so this band must be reassigned to a higher complex. The sharp 1127.1 cm^{-1} band and 1417.4 cm^{-1} feature increase on early annealing cycles and then decrease, the sharp 1401.6 and 1684.2 cm^{-1} bands increase steadily, and the 2585.3 (not shown), 1498.4, 1442.8, and 680 cm^{-1} absorptions increase markedly while the above 1:1 complex bands decrease on successive annealing cycles (Figure 4). Ultraviolet irradiation after 30 K annealing slightly decreases the bands associated with all complexes, $(HI)_2$, and $(HI)_3$ and

TABLE 4: Bond Lengths (Å), Frequencies (cm^{-1}), and Intensities (km/mol) Calculated for H_3N-HI Complexes in C_{3v} Symmetry Using Density Functional Theory[a]

B3LYP	∠HN−H: 110.8° (μ = 4.71 D) more covalent
H−N: 1.0157	minimum[b,c] 3598 (e, 16), 3473 (a_1, 1), 1726 (a_1,
N−H: 1.8454	1703), 1657 (e, 29), 1087 (a_1, 93), 657 (e, 30), 224
H−I: 1.6649	(e, 23), 129 (a_1, 40)[d]
B3LYP	∠HN−H: 109.8° (μ = 7.46 D) transition state[b]
H−N: 1.0170	3588 (e, 44), 3458 (a_1, 5), 1641 (e, 40), 1201 (a_1,
N−H: 1.3818	267), 1108 (e, 14), 431 (a_1, 830), 307 (e, 11), 481i
H−I: 1.8505	(a_1, 3626)
B3LYP	∠HN−H: 109.4° (μ = 9.06 D) more ionic minimum[b]
H−N: 1.0186	3569 (e, 66), 3442 (a_1, 5), 1638 (e, 33), 1310 (e, 12),
N−H: 1.2161	1298 (a_1, 585), 869 (a_1, 3727), 319 (e, 134), 296
H−I: 1.9968	(a_1, 8)[e]
BPW91	∠HN−H: 109.8° (μ = 7.71 D) proton shared minimum
H−N: 1.0225	3529 (e, 43), 3393 (a_1, 3), 1602 (e, 33), 1169 (a_1,
N−H: 1.3650	320), 1107 (e, 12), 596 (a_1, 3113), 301 (e, 13), 211
H−I: 1.8734	(a_1, 759)
B3LYP	∠HN−H: 109.5° (μ = 11.0 D) still more ionic
H−N: 1.0208	minimum[f] 3545 (96), 3540 (102), 3428 (20), 1865
N−H: 1.1273	(100), 1848 (4118), 1842 (110), 1428 (24), 1413
H−I: 2.1362	(27), 1335 (0.1), 342 (8), 267 (109), 120 (14)
B3LYP	ammonia (∠H−N−H: 108.0°, μ = 1.68 D) and
H−N: 1.0140	hydrogen iodide (μ = 0.88 D)
H−I: 1.6066	NH_3: 3614 (e, 4), 3486 (a_1, 2), 1668 (e, 29),
	998 (a_1, 215)
	HI: 2307.9 (4.3)[g]

[a] The 6-311++G(d,p) basis and LANL2DZ pseudopotential were used for all calculations. [b] Energies −6.6, −5.8, and −6.0 kcal/mol, respectively, relative to NH_3 + HI. [c] The 6-311+G(d,p) basis set gave the same H−N length (N−H, 1.8483 Å; H−I, 1.6659 Å) and the same frequencies ±2 cm^{-1} except the strongest band was 9 cm^{-1} lower. At this level, the complex is bound by 6.5 kcal/mol. [d] ^{15}N-isotopic shifts in order are 9.9, 2.2, 0.0, 3.3, 5.2, 1.0, 0.2, and 3.2 cm^{-1}; D-isotopic frequencies in order are 2650, 2479, 1227, 1203, 831, 474, 161, and 119 cm^{-1}. [e] ^{15}N-isotopic shifts in order are 11.1, 2.0, 2.1, 3.6, 8.3, 1.0, 7.2, and 0.3 cm^{-1}. [f] SCIPCM in heptane solution. [g] DI: 1639.0 (2.2 km/mol).

increases NH_3 monomer and HI monomer bands by 60%; such photodissociation of HI complexes has been investigated.[39]

Evidence has been presented in our investigation on the NH_4-Br system[23] for sharp bands near 1400 and 1730 cm^{-1}, which are close to ν_4 and $\nu_4 + \nu_6$ for solid NH_4Br;[35] these bands show the same 6.1 cm^{-1} ^{15}N-shift and are assigned to the same modes (antisymmetric NH_4^+ bending fundamental and combination with the ammonium ion torsional mode) in a small ionic cluster. In our NH_4I experiments, sharp 1401.8 and 1684.2 cm^{-1} bands exhibit identical relative increases on annealing cycles and must be assigned to an analogous species. In the present case, the ^{15}N-shifts of each band are an identical 6.2 cm^{-1}, which is appropriate for the ν_4 ammonium ion fundamental; the ν_6 torsion about the central nitrogen should exhibit no ^{15}N-shift; hence, the $\nu_4 + \nu_6$ combination band has the same ^{15}N-shift as the ν_4 fundamental. The solid spectrum after 45 K annealing reveals 1404.0 and 1684.8 cm^{-1} bands for ν_4 and $\nu_4 + \nu_6$ of solid NH_4I, which are in good agreement with literature spectra.[35,36] Note that the NH_4^+ torsional fundamental in solid NH_4I (1684.8 − 1404.0 = 280.8 cm^{-1}) and that in the argon matrix-isolated complex (1684.2 − 1401.8 = 282.4 cm^{-1}) are nearly the same. These values are 335 and 334.0 cm^{-1}, respectively, for the NH_4-Br species.[23,35]

The 1127.1 cm^{-1} band that increases first and then decreases on annealing cycles while the 1:1 complex decreases and higher *x*:*y* complexes increase is assigned to the 1:2 complex. This feature is a perturbed ν_2 ammonia motion as suggested by the 5.4 cm^{-1} shift, and the resolved 1127.1 and 1121.7 cm^{-1} doublet in the mixed $^{14}N/^{15}N$ isotopic experiment shows that a single NH_3 subunit is involved. Similar 1:2 complexes have been observed at 1089.2 and 1111.2 cm^{-1} in the HCl and HBr systems. The 2585, 1498, 1442, and 680 cm^{-1} bands increase on annealing and are due to higher complexes.

The new isotopic data reported here allow further characterization of the absorption bands due to the 1:1 complex and require a reassignment of the vibrational modes. First, the 3400 cm^{-1} band gives a sharp 3400.1−3391.8 cm^{-1} doublet in the mixed $^{14}N/^{15}N$ isotopic experiment characterizing the vibration of a single ammonia subunit. In addition, the 606, 592 cm^{-1} site split band appears as a doublet with ^{15}N-counterparts at 603, 589 cm^{-1} suggesting the participation of a single N atom. The broader 1259 and 875 cm^{-1} features give unresolved 1257 and 874 cm^{-1} bands, which suggest 4 and 2 cm^{-1} ^{15}N-shifts, respectively, for these bands. Our ND_4I experiments reveal a 2534.2 cm^{-1} counterpart for the 3400.1 cm^{-1} absorption, which substantiates its assignment as the antisymmetric NH_3 stretching mode in the H_3N-HI complex. The strongest band at 1256 cm^{-1} (here 1259 cm^{-1}) was first assigned to the H−I stretching mode in the 1:1 complex,[10] but this band must be reassigned to the perturbed symmetric NH_3 bending mode. The 4 cm^{-1} ^{15}N-shift deduced here is in agreement with the 4.3 cm^{-1} ^{15}N-shift observed for the analogous 1146.7 cm^{-1} band of the H_3N-HBr complex. The H/D ratio (Schriver 1256/1005 = 1.250, this work 1259/1004 = 1.254) is in near agreement with that for H_3N-HBr (1146.7/906.6 = 1.265) and ammonia (974.6/759.7 = 1.283).[23] Furthermore, the *same* 1256 cm^{-1} band was observed by Schriver with NH_3/HI and with NH_3/DI and this abnormal isotopic distribution was rationalized by exchange between DI and NH_3 in the matrix.[11] Here, NH_3/DI experiment reveals virtually no extra absorption at 1005 cm^{-1} on the side of NH_3 where D_3N-DI and $(NH_3)_2$ also absorb and the sample shows little evidence of isotopic exchange. Reassignment of the 1256 cm^{-1} band as the NH_3 mode instead of the H−I mode easily explains the NH_3/DI spectrum.[11] Finally, the observation of four mixed H/D bands at 1255, 1138, 1081, and 1008 cm^{-1} with relative intensities tracking the NH_3, NH_2D, NHD_2, and ND_3 bands at 975, 911, 844, and 760 cm^{-1} supports the symmetric ammonia bending description of this mode.

The 590 cm^{-1} band (here 606, 592 cm^{-1} doublet) was first assigned to the hydrogen bond bending mode and then to the ammonia rocking mode.[8,10] Our DFT calculation rules out the latter possibility, and we prefer 875 cm^{-1} for the bending mode; the approximately 2 cm^{-1} ^{15}N-shift is in accord. We believe the 592 cm^{-1} band is better reassigned to the antisymmetric N−H−I vibration. The 3 cm^{-1} ^{15}N-shift supports this assignment as the analogous 729.3 cm^{-1} mode for $H_3N-H-Br$ exhibits a 3.8 cm^{-1} ^{15}N-shift.[23] The weak 432 cm^{-1} band is probably due to the D_3N-DI counterpart; the 592/432 = 1.37 ratio is typical for such motions. In the shared proton system $(I-H-I)^-$, the antisymmetric stretching mode at 682 cm^{-1} shows a 682/420 = 1.45 H/D frequency ratio.[41] The proximity of the $I-H-I^-$ and H_3N-H-I modes supports this characterization. The neon matrix shift to be discussed below confirms this reassignment.

Neon. Assignment of the product absorptions in solid neon follows the above rationale for the analogous argon matrix bands. The 1:1 complex absorptions are at 3435.3, 1192.5, and 630 cm^{-1} in solid neon; these bands decrease slightly on annealing while higher complex absorptions increase (Figure 1). The 3425.3 cm^{-1} absorption with 3426.5 and 2558.3 cm^{-1} ^{15}N and D isotopic counterparts is clearly due to the antisymmetric NH_3 stretching mode in the H_3N-HI complex. The 1192.5 cm^{-1} band shows a 5 cm^{-1} ^{15}N-shift and a 1192.5/960.3 = 1.242 H/D ratio, which are characteristic of a symmetric NH_3 bending mode. Note the neon matrix perturbation from NH_3 is

less (224.3 cm^{-1}) than that for more strongly interacting argon (284 cm^{-1}). If these were H−I stretching modes, the neon counterpart would be higher (less displaced from HI); thus the neon−argon shift supports the present NH_3 mode assignment. The mixed H/D precursor gives 1130 and 1044 cm^{-1} intermediate bands for the 1192 cm^{-1} absorption and confirms the NH_3 bending character of this mode. The strong 630 cm^{-1} band is assigned to the antisymmetric N−H−I stretching mode; the 4 cm^{-1} ^{15}N-shift and 630/473 = 1.322 H/D ratio substantiate this assignment.

Neon/Argon Mixtures. The mixed neon/argon matrix experiments with 0.2, 1, 2, and 5% Ar in Ne clearly show the evolution of absorptions from the neon to argon matrix positions on increasing Ar concentration and on annealing to allow diffusion. Even with very small mole percents of argon present, the argon interaction dominates. This is most clearly demonstrated on annealing (Figure 5b−e) where diffusion allows argon atoms to replace neon atoms in the intimate coordination sphere around the polar H_3N−HI complex. Note that the NH_3 submolecule modes (3435 and 1192 cm^{-1} in neon) are more sensitive to the argon interaction than the HI submolecule mode (630 cm^{-1} in neon). Also note that the 1:2 band at 1138.0 cm^{-1} in neon red shifts in argon (to 1127.1 cm^{-1}) in contrast to the above blue shift for the 1192 cm^{-1} 1:1 complex absorption. This suggests that proton transfer in the 1:2 complex is less vulnerable to solvent effects than proton transfer in the 1:1 complex.

Krypton. The krypton matrix studies confirm the environmental trend from neon to argon, which shifts the antisymmetric N−H−I stretching mode to the red (630 to 592 to 520 cm^{-1}), the symmetric NH_3 bending mode to the blue (1192 to 1259 to 1277 cm^{-1}), and the antisymmetric NH_3 stretching mode to the red (3435 to 3400 to 3387 cm^{-1}), and support the present mode assignments for the H_3N−HI complex. Notice that these changes are not uniform: the neon to argon environmental change affects the NH_3 submolecule modes more, but the argon to krypton host change red shifts the N−H−I mode more and broadens the band. This low 520 cm^{-1} frequency must involve a nearly equally shared proton.

Nitrogen. The present experiment codepositing dilute NH_3/HI and ND_3/DI from thermal decomposition of ammonium iodide with excess N_2 at 5 K produces first on annealing the same 1:1 complex bands (Figures 6 and 7) reported by Schriver et al.[10,11] and higher complex bands, with the assignments described above. The 1955 cm^{-1} band is stronger here, and we identify it as the major site for the H_3N−HI complex. We deduce a 4 cm^{-1} ^{15}N-shift for this band and measure 5.1, 4, and 8 cm^{-1} ^{15}N-shifts for the associated 1408.6, 1626.7, and 3390.4 cm^{-1} absorptions.[42] The latter band is due to the antisymmetric NH_3 stretching mode, which exhibits a 2521.6 cm^{-1} band with ND_4I and broad 3386 and 2522 cm^{-1} mixed H/D counterparts. The 1626.7 cm^{-1} band is near the antisymmetric bending mode of NH_3, and this mode must be assigned accordingly; the apparent deuterium counterpart at 1254.7 cm^{-1} is, however, higher than the ND_3 absorption. Our mixed H/D sample provides NH_2D and NHD_2 counterparts at 1576, 1448, 1389, and 1286 cm^{-1} in support of this assignment. The 1408.6 cm^{-1} band exhibits the ^{15}N-shift for a symmetric ammonia bending mode and is considerably blue-shifted by the strong hydrogen bonding interaction and approaches an ammonium ion mode. The 1967−1925 cm^{-1} absorptions for H_3N−HI were first assigned to the H−I stretching mode,[10] and then the 1540−1530 cm^{-1} D_3N−DI counterparts were described as an antisymmetric N−D−I motion;[11] here, we continue this evolution and simply characterize the 1955 cm^{-1} band as the N−H stretching mode in the H_3N−HI complex with substantial proton transfer sustained by strong interaction with the nitrogen matrix host. The mixed H/D observations of Schriver show a small secondary deuterium dependence for this mode (to 1940 and to 1910 cm^{-1}), and our mixed H/D spectrum reveals a broad 1955, 1920, 1903, 1878 cm^{-1} quartet which demonstrates the primary involvement of the hydrogen-bonded proton and the secondary involvement of a NH_3 subgroup. Furthermore, the deduced 4 cm^{-1} ^{15}N-shift is in agreement with the N−H stretching characterization. This frequency is 1955/3170 = 0.62 of a 3170 cm^{-1} representative frequency for the $N-H^+$ stretching mode.[8] The low H/D = 1955/1527 = 1.280 ratio arises from anharmonicity in this strong hydrogen-bonded system.[43]

The sharp, weaker band observed here at 1894.1 cm^{-1} (Figure 7) is probably due to D_3N−HI although there is insufficient hydrogen population in the HI and the NHD_2 impurity even with rearrangement in the complex[11] to account for the 1894.1 cm^{-1} band intensity relative to 1538.5, 1527.6 cm^{-1}. Hence, we suggest that the N−H stretching mode in these ionic H_3N−HI complexes is stronger relative to the N−D mode than expected. Finally, the weak 1557.1 cm^{-1} band relates to the 1538.5, 1527.6 cm^{-1} bands for D_3N−DI as the NHD_2 intensity does to ND_3, and the 1557.1 cm^{-1} band is assigned to HD_2N−DI.

The 1847 cm^{-1} band was first assigned to a site of the H−I stretching mode and then to a combination band of the 1627 cm^{-1} NH_3 submolecule bending mode and a lower frequency 250 cm^{-1} fundamental in Fermi resonance with the 1967 cm^{-1} band.[10,11] However, the weaker 1371.0 cm^{-1} 1:1 complex band and 1380.9 cm^{-1} satellite in ND_4I experiments need a hydrogen counterpart, and the 1847−1831 cm^{-1} band is appropriate. The present experiments reveal no ^{15}N-shift for the latter band, which means that the ^{15}N-shift is less than 1 cm^{-1}, and opens the possibility that this is the degenerate N−H−I bending mode. The 1831/1371 = 1.336 ratio is appropriate for this reassignment. The mixed isotopic experiments are also in accord with this reassignment as the 1831 cm^{-1} band becomes 1792, 1772, and 1767 cm^{-1} with NH_2D, NHD_2, and ND_3 present in the sample.

Calculations. While DFT calculations on HI and H_3N−HI are only approximations, some useful frequency trends are provided. First, the computed harmonic frequency and bond length for HI are within 1 cm^{-1} and 0.003 Å of the observed values.[44] On the basis of near agreement between the calculated (3.510 Å) and observed[15] (3.584 Å) N−H−I distances for the ground-state complex, the B3LYP functional provides a realistic prediction of gas-phase frequencies. The calculated H−I fundamental (1726 cm^{-1}) is 0.75 of the value calculated for HI itself (2308 cm^{-1}), and the calculated symmetric NH_3 mode in the complex (1087 cm^{-1}) is 1.089 times the ammonia value (998 cm^{-1}). The calculated dipole moment represents a transfer of 0.28 e from N to I in the absence of polarization. On the other hand, the BPW81 functional overestimates the degree of proton transfer and produces a N−H−I bond that is too short, but the strong calculated a_1 frequencies of 1169 cm^{-1} (sym NH_3) and 596 cm^{-1} (antisym N−H−I) are good approximations to the neon (1192, 630 cm^{-1}) and argon (1259, 592 cm^{-1}) matrix values where interaction with neon and argon in turn has increased the degree of proton transfer from that found in the gas phase.[14,15] The BPW91 calculated dipole moment (7.71 D) in the absence of polarization would correspond to a transfer of 0.50 e from N to I. The B3LYP functional also converges a 0.63 kcal/mol higher energy, more ionic minimum on the potential energy surface. This structure has a calculated

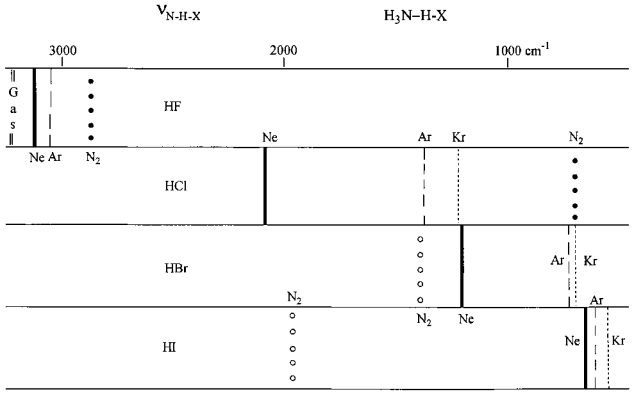

Figure 9. Display of N−H−X stretching frequencies (from H−X to N−H) for H_3N-HX complexes in solid neon, argon, krypton, and nitrogen matrices (open circles note N−H stretch).

predominantly N−H stretching mode at 869 cm^{-1} and a symmetric NH_3 mode at 1298 cm^{-1}. The calculated dipole moment represents a transfer of 0.58 e from N to I. If the frequency changes from the first more covalent to the second more ionic complex are continued, the frequencies observed in solid nitrogen (1955 cm^{-1} N−H stretch, 1409 cm^{-1} NH_3 bending) will be attained, which are characteristic of substantial proton transfer.

The SCIPCM calculation for H_3N-HI in heptane solution produces an interesting result. The N−H = 1.1273 Å length is the shortest; the proton transfer is therefore more complete, and the dipole moment is the highest value found here. The 11.0 D dipole moment represents the transfer of 0.70 e from N to I. The computed frequencies are physically reasonable although degeneracy is reduced and the NH_3 bending modes are calculated about 180 cm^{-1} higher than those for NH_3 itself. The very strong computed 1848 cm^{-1} band is essentially an N−H stretching mode, and this mode approaches the 1955 cm^{-1} band observed in solid nitrogen. Furthermore, the computed 267 cm^{-1} H_3NH-I stretching mode is near the 250 cm^{-1} band observed by Schriver in solid nitrogen and assigned to the H−I librational mode.[11] Our calculation suggests reassigning this band to the H_3NH-I stretching mode.

Bonding Trends. Two interesting trends are at work here: the chemical relationship among NH_3 complexes with HF, HCl, HBr, and HI with decreasing proton dissociation energies and the physical solvation effect of neon, argon, krypton, and nitrogen matrix hosts on vibrational spectra. First, the gas-phase complexes in the ground vibrational state have small, increasing ionic character in this series and are adequately described as simple hydrogen-bonded complexes.[15,16] Second, the vibrational absorption spectra probe the more polar first vibrational level, and the trends are summarized in Figure 9 which illustrates the N−H−X vibrational mode. For HF, this mode is H−F stretching with virtually no nitrogen involvement,[9] the high ionic dissociation energy of HF renders the H_3N-HF complex immune to significant matrix effects, and the Ne to Ar to N_2 frequencies summarized in Table 5 are slightly below the 3220 ± 10 cm^{-1} gas-phase value.[18] There is a substantial decrease in dissociation energies for HCl, HBr, and HI, and as a direct consequence, proton transfer becomes easier energywise and small solvent effects can play a greater role in assisting this process. For HCl, the 2084 cm^{-1} neon matrix H−Cl stretching mode is believed to be only slightly red-shifted from the yet-to-be-determined gas-phase value,[19] but the argon and krypton values are substantially shifted and the nitrogen host frequency is further shifted to 702 cm^{-1} where this mode is characterized as antisymmetric N−H−Cl stretching.[5,6,19] For HBr, even the neon matrix H−Br mode is shifted below reasonable predictions of the gas-phase frequency[22,23] and the argon matrix 729 cm^{-1} fundamental is described as antisymmetric N−H−Br stretching,[8,23] but now the nitrogen host helps support more proton transfer and the 1392 cm^{-1} band is mostly a N−H stretching mode.[23] For HI, the neon matrix band at 630 cm^{-1} is N−H−I stretching and proton transfer is even more in the nitrogen host giving a 1955 cm^{-1} N−H stretching mode, which is 62% of the 3170 cm^{-1} reference $N-H^+$ value.[8] Accordingly, as the degree of proton transfer increases, the H−X frequency decreases to a minimum and then increases as a N−H stretching mode. It is clear from the nitrogen matrix frequencies that H_3N-HI is more ionic than H_3N-HBr. The nitrogen matrix environment is well-known for stabilizing and shifting ionic species (LiO and LiO_2, for example).[45,46] These trends have been summarized in vibrational correlation diagrams by two groups.[7,8] The matrix environment has a profound effect on the vibrational spectra of polar complexes, and the neon−argon matrix shift can be used to help characterize the vibrational mode.

TABLE 5. Frequencies (cm^{-1}) Assigned to Ammonia−Hydrogen Halide Complexes in Solid Matrices

	H−X stretch	sym NH_3 bend	H−X bend	asym NH_3 stretch
H_3N-HF in Ne	3106	1090	912	
Ar	3041	1093	916	
N_2	2778	1110	1023	
H_3N-HCl in Ne[a]	2084	1060	709	
Ar[a,b]	1371	1070	734	3430
Kr[a]	1218	1072	737	3420
N_2[a−c]	702	1251	628?	3420
H_3N-HI in Ne	1209	1080		3445
Ar[d]	729	1146	591	3421
Kr	700	1188	624	3407
N_2	1392[e]	1212[e]		3403
H_3N-HI in Ne	630	1192		3435
Ar[f]	592[g]	1259[g]	875	3400
Kr	520	1277		3387
N_2[f]	1955[h]	1409		3391

[a] Reference 16. [b] Reference 6. [c] Reference 5. [d] Reference 8. [e] The 1392 cm^{-1} band is reassigned to the predominately N−H stretching mode and the 1212 cm^{-1} band to the largely symmetric ammonia bending mode in the H_3N-H-I complex; these two a_1 modes are mixed coordinates. [f] Reference 10. [g] Reassignments, this work. [h] The 1955 cm^{-1} band is characterized here as a predominately N−H stretching mode.

Conclusions

Ammonia and hydrogen iodide vapors from the thermal decomposition of NH_4I were codeposited with excess neon at 5 K to form the H_3N-HI complex. New 630, 1192, and 3435 cm^{-1} infrared absorptions are assigned to the antisymmetric N−H−I stretching, symmetric NH_3 bending, and antisymmetric NH_3 stretching modes of the 1:1 complex. The neon matrix spectrum suggests a strong hydrogen bond, considerably stronger than in the gas-phase complex, owing to solvation by the matrix. Complementary experiments were done with argon, krypton, and nitrogen to investigate the 1:1 complex in a range of matrix environments and to compare with previous work using the reagent gases. The above modes are shifted to 592, 1259, and 3400 cm^{-1} in solid argon and to 1955 (now N−H stretching), 1409, and 3391 cm^{-1} in solid nitrogen owing to an increased interaction with the matrix and the resulting increased proton transfer. Neon−trace argon mixtures gave intermediate absorptions, which evolved to the pure argon values on annealing and showed that argon replaces neon in the solvating shell; these

experiments provide evidence for diffusion of the matrix atoms on annealing the solid. These and earlier[10,11] matrix isolation experiments show that the matrix environment markedly affects the hydrogen bonding interaction and the degree of proton transfer in this polar H_3N-HI hydrogen-bonded complex.

Acknowledgment. We gratefully acknowledge financial support from National Science Foundation Grant 00-78836 and computer time from the San Diego Supercomputer Center.

References and Notes

(1) Clementi, E. *J. Chem. Phys.* **1967**, *46*, 3851; *47*, 2323.
(2) Raffenetti, R. C.; Phillips, D. H. *J. Chem. Phys.* **1979**, *71*, 4534.
(3) Latajka, Z.; Scheiner, S. *J. Chem. Phys.* **1984**, *81*, 4014. Latajka, Z.; Scheiner, S.; Ratajczak, H. *Chem. Phys Lett.* **1987**, *135*, 367.
(4) Brciz, A.; Karpfen, A.; Lischka, H.; Schuster, P. *Chem. Phys.* **1984**, *89*, 337.
(5) Ault, B. S.; Pimentel, G. C. *J. Phys. Chem.* **1973**, *77*, 1649.
(6) Barnes, A. J.; Beech, T. J.; Mielke, Z. *J. Chem. Soc., Faraday Trans. 2* **1984**, *80*, 455.
(7) Ault, B. S.; Steinbach, E.; Pimentel, G. C. *J. Phys. Chem.* **1975**, *79*, 615.
(8) Barnes, A. J.; Wright, M. P. *J. Chem. Soc., Faraday Trans. 2* **1986**, *82*, 153.
(9) Johnson, G. L.; Andrews, L. *J. Am. Chem. Soc.* **1982**, *104*, 3043.
(10) Schriver, L.; Schriver, A.; Perchard, J. P. *J. Am. Chem. Soc.* **1983**, *105*, 3843.
(11) Schriver, L. *Spectrochim. Acta* **1987**, *43A*, 1155.
(12) Howard, N. W.; Legon, A. C. *J. Chem. Phys.* **1987**, *86*, 6722.
(13) Howard, N. W.; Legon, A. C. *J. Chem. Phys.* **1988**, *88*, 4694.
(14) Legon, A. C.; Stephenson, D. *J. Chem. Soc., Faraday Trans.* **1992**, *88*, 761.
(15) Legon, A. C. *Chem. Soc. Rev.* **1993**, 153 and references therein.
(16) Barnes, A. J.; Legon, A. C. *J. Mol. Struct.* **1998**, *448*, 101.
(17) Andrews, L. In *Chemistry and Physics of Matrix Isolated Species*; Andrews, L., Moskovits, M., Eds.; Elsevier: Amsterdam, 1989; Chapter 2.
(18) Thomas, R. K. Personal communication, 1981 (unpublished 3215 cm^{-1} absorption for H−F mode in H_3N-HF complex). Miller, R. E. Personal communication, 2001 (unpublished 3230 cm^{-1} fundamental). See Miller, R. E. *Science* **1988**, *240*, 447.
(19) Andrews, L.; Wang, X.; Mielke, Z. *J. Am. Chem. Soc.* **2001**, *123*, 1499; *J. Phys. Chem. A* **2001**, *105*, 6054.
(20) Del Bene, J. E.; Jordan, M. J. T.; Gill, P. M. W.; Buckingham, A. D. *Mol. Phys.* **1997**, *92*, 429.
(21) Del Bene, J. E.; Jordan, M. J. T. *J. Chem. Phys.* **1998**, *108*, 3205.
(22) Jordan, M. J. T.; Del Bene, J. E. *J. Am. Chem. Soc.* **2000**, *122*, 2101.
(23) Andrews, L.; Wang, X. *J. Phys. Chem. A* **2001**, *105*, 6420.
(24) Vapor pressure 2−15 mTorr. *Handbook of Chemistry and Physics*; Chemical Rubber Publishing Co.: Cleveland, OH, 1968; p D-139.
(25) Suzer, S.; Andrews, L. *J. Chem. Phys.* **1987**, *87*, 5131.
(26) Frisch, M. J.; Trucks, G. W.; Schlegel, H. B.; Scuseria, G. E.; Robb, M. A.; Cheeseman, J. R.; Zakrzewski, V. G.; Montgomery, J. A., Jr.; Stratmann, R. E.; Burant, J. C.; Dapprich, S.; Millam, J. M.; Daniels, A. D.; Kudin, K. N.; Strain, M. C.; Farkas, O.; Tomasi, J.; Barone, V.; Cossi, M.; Cammi, R.; Mennucci, B.; Pomelli, C.; Adamo, C.; Clifford, S.; Ochterski, J.; Petersson, G. A.; Ayala, P. Y.; Cui, Q.; Morokuma, K.; Malick, D. K.; Rabuck, A. D.; Raghavachari, K.; Foresman, J. B.; Cioslowski, J.; Ortiz, J. V.; Stefanov, B. B.; Liu, G.; Liashenko, A.; Piskorz, P.; Komaromi, I.; Gomperts, R.; Martin, R. L.; Fox, D. J.; Keith, T.; Al-Laham, M. A.; Peng, C. Y.; Nanayakkara, A.; Gonzalez, C.; Challacombe, M.; Gill, P. M. W.; Johnson, B. G.; Chen, W.; Wong, M. W.; Andres, J. L.; Head-Gordon, M.; Replogle, E. S.; Pople, J. A. *Gaussian 98*, revision A.1; Gaussian, Inc.: Pittsburgh, PA, 1998.
(27) (a) Becke, A. D. *Phys. Rev. A* **1988**, *38*, 3098. (b) Perdew, J. P.; Wang, Y. *Phys. Rev. B* **1992**, *45*, 13244.
(28) (a) Becke, A. D. *J. Chem. Phys.* **1993**, *98*, 5648. (b) Lee, C.; Yang, W.; Parr, R. G. *Phys. Rev. B* **1988**, *37*, 785.
(29) (a) Krishnan, R.; Binkley, J. S.; Seeger, R.; Pople, J. A. *J. Chem. Phys.* **1980**, *72*, 650. (b) Frisch, M. J.; Pople, J. A.; Binkley, J. S. *J. Chem. Phys.* **1984**, *80*, 3265.
(30) Hay, P. J.; Wadt, W. R. *J. Chem. Phys.* **1985**, *82*, 270. Wadt, W. R.; Hay, P. J. *J. Chem. Phys.* **1985**, *82*, 284. Hay, P. J.; Wadt, W. R. *J. Chem. Phys.* **1985**, *82*, 299.
(31) Abouaf-Marguin, L.; Jacox, M. E.; Milligan, D. E. *J. Mol. Spectrosc.* **1977**, *67*, 34.
(32) Bowers, M. T.; Flygare, W. H. *J. Chem. Phys.* **1966**, *44*, 1389.
(33) Barnes, A. J.; Davies, J. B.; Hallam, H. E.; Howells, J. D. R. *J. Chem. Soc., Faraday Trans. 2* **1973**, *69*, 246.
(34) Engdahl, A.; Nelander, B. *J. Phys. Chem.* **1986**, *90*, 6118.
(35) Wagner, E. L.; Hornig, D. F. *J. Chem. Phys.* **1950**, *18*, 305.
(36) Vedder, W.; Hornig, D. F. *J. Chem. Phys.* **1961**, *35*, 1560 and references therein.
(37) Perchard, J. P.; Schriver, A.; Schriver, L. *J. Mol. Struct.* **1987**, *156*, 75.
(38) Foresman, J. B.; Keith, T. A.; Wiberg, K. B.; Snoonian, J.; Frisch, M. J. *J. Phys. Chem.* **1996**, *100*, 16098.
(39) Schriver, L.; Schriver, A.; Perchard, J. P. *J. Mol. Struct.* **1990**, *222*, 141.
(40) Tao, F.-M. *J. Chem. Phys.* **1999**, *110*, 11121.
(41) Noble, P. N. *J. Chem. Phys.* **1972**, *56*, 2088. Ellison, C. M.; Ault, B. S. *J. Phys. Chem.* **1979**, *83*, 832.
(42) We measure a 4 cm^{-1} ^{15}N-shift for the sharp 1925 cm^{-1} band, which is not overlapped by other site absorptions.
(43) Guissani, Y.; Ratajczak, H. *Chem. Phys.* **1981**, *62*, 319.
(44) Huber, K. P.; Herzberg, G. *Constants of Diatomic Molecules*; Van Nostrand Reinhold: New York, 1979.
(45) Andrews, L. *J. Chem. Phys.* **1969**, *50*, 4288.
(46) Spiker, R. C., Jr.; Andrews, L. *J. Chem. Phys.* **1973**, *58*, 702.